ELSEVIER

Journal of Nuclear Materials 270 (1999) 265–272

journal of nuclear materials

Effect of particle size on the diffusion behavior of some radionuclides in compacted bentonite

Tamotsu Kozaki [a], Yuichi Sato [a], Mamoru Nakajima [a,b], Hiroyasu Kato [c], Seichi Sato [a], Hiroshi Ohashi [a,*]

[a] *Division of Quantum Energy Engineering, Graduate School of Engineering, Hokkaido University, Sapporo 060-8628, Japan*
[b] *Japan Nuclear Fuel Limited, Fukokuseimei BLDG., 2-2-2, Uchisaiwai-cho, Chiyoda-ku, Tokyo 100-0011, Japan*
[c] *Energy and Ecosystem Laboratories, Central Research Institute, Mitsubishi Materials Corporation, 1002-14 Mukoyama, Naka-machi, Naka-gun, Ibaraki-ken 311-0102, Japan*

Received 7 May 1998; accepted 22 September 1998

Abstract

For performance assessment of bentonite buffer material in geological disposal of high-level radioactive waste, the particle size of bentonite and its effect on the diffusion behavior of radionuclides in compacted bentonite were studied. Bentonite samples with different particle sizes were prepared, and characterized by the BET and EGME methods for specific surface areas, by the laser diffraction/scattering particle size analysis for particle size distribution, and by SEM observations. Apparent and effective diffusion coefficients of tritiated water (HTO), Cl^- ions and Cs^+ ions in compacted bentonite were also determined using bentonite samples with different particle sizes. With HTO and Cl^- ions, there were higher diffusion coefficients in fine grained samples, but opposite particle size effects were observed with Cs^+ ions. These findings cannot be explained by the conventional pore water diffusion model, and suggest a different diffusion process for Cs^+ ions and also at higher dry density region.

1. Introduction

Compacted bentonite is a candidate for buffer material in geological disposals of high-level radioactive waste [1,2]. An important function of the compacted bentonite is to retard the transport of radionuclides from the waste forms to the surrounding host rock in a repository. It is therefore necessary to study the migration behavior of radionuclides in compacted bentonite, especially the diffusion behavior of radionuclides in compacted bentonite, since compacted bentonite has very low permeability and the diffusion governs the transport of radionuclides in the system.

Based on the extensive studies of the diffusion behavior, a pore water diffusion model has been widely adopted to interpret the experimental results of the diffusion of radionuclides in compacted bentonite [3–5]. In this model, it is considered that the radionuclides diffuse in the pore water, and both the geometrical structure of pores and sorption of radionuclides on bentonite can affect their diffusion coefficients. However, some reports [6–11] have noted discrepancies between the experimental data and model calculations, and have attributed the discrepancies to the contribution of surface diffusion, which would mean that radionuclides sorbed on clay migrate on the clay surfaces. Oscarson et al. [12] have pointed out that the discrepancies can be attributed to decreases in distribution coefficients at high dry densities and that surface diffusion is not predominant for clay with dry densities below 1.6 Mg m^{-3}. The authors here studied the activation energies for diffusion and suggested the possible contribution of several diffusion processes in the system [13–16]. At the present time, however, diffusion phenomena are not fully understood.

The geometrical structure of pores is important to understand diffusion phenomena. Although the effective size of pores in compacted bentonite has been theoretically estimated by introducing the electrical double layer theory to the gaps between bentonite particles [17–19], there are no reports available on the relationship be-

* Corresponding author. Tel.: +81-11 706 6686; fax: +81-11 706 7139; e-mail: ohashi@qe.eng.hokudai.ac.jp.

0022-3115/99/$ – see front matter
PII: S0022-3115(98)00782-X

tween the particle size of clay minerals and the formation factor in the compacted bentonite. In this study, we focused on the particle size of bentonite, which is considered to be closely related to the formation factor in the pore water diffusion model. Two bentonite samples with different particle sizes were prepared and characterized by several methods. In addition, diffusion coefficients of tritiated water (HTO), Cl^- ions, and Cs^+ ions in water-saturated, compacted bentonite were determined, and the effect of the particle size on the diffusion behavior was discussed.

2. Experimental

2.1. Preparation and characterization of sample

The bentonite sample used in this study was Kunipia-F, a product of Kunimine Industries. The montmorillonite content of Kunipia-F is over 95 wt% [5]. The bentonite was purified by both agitation in NaCl solution and settlement: ten grams of Kunipia-F were added to 1 dm^3 of 1 M NaCl solution and agitated for 24 h. The montmorillonite suspension was then allowed to settle for 24 h and the supernatant was exchanged with new NaCl solution. Both agitation and settlement were repeated three times. Excess salt was removed with a dialysis tube (Viskase Sales, UC36-32-100) in distilled water. The distilled water was renewed every two or three days until no chloride was detected with $AgNO_3$. The purified montmorillonite was dried in an oven at 378 K and then mortared with a pestle and sieved to obtain samples with coarse (particle size 75–150 μm) and with fine particle sizes (particle size <45 μm).

Specific surface areas were measured for both samples by the BET (N_2 gas adsorption) method using Quantasorb (Yuasa Ionics), and by the EGME (ethyleneglycolmonoethylether) method [20]. The bentonite particles were observed by scanning electron microscopy (JEOL, JSM-T20), and particle size distributions were determined by laser diffraction/scattering particle size analysis (Cilas, type-1064). The bentonite samples for the particle size analyzer were prepared by dispersing them either in ethanol alone or in water with sodium hexametaphosphate, $Na_6(PO_3)_6$, using ultrasonic vibrations for 60 min. The solid/liquid ratio of the dispersed samples was 0.01 g cm^{-3}.

2.2. Diffusion experiments

2.2.1. Non-steady diffusion experiment

In one-dimensional non-steady diffusion experiments, the bentonite powder was compacted in an acrylic resin cell (20-mm diameter by 20-mm thickness) to a dry density of 1.0 or 1.8 Mg m^{-3}, and saturated with distilled water by contact through sintered stainless steel filters at room temperature for about 30 d. A small amount of tracer solution (HTO, ^{36}Cl or ^{134}Cs) was applied to one end of the bentonite specimen after the water-saturation. The tracer was allowed to diffuse in the bentonite sample at 298 K for a given period from 6 to 1346 h by placing two bentonite specimens in contact, as shown in Fig. 1. After diffusion, the cell was disassembled and the bentonite specimen was sectioned into 0.5-mm-thick slices as the specimen was extruded from the cell in steps. The thickness of the slices had been previously confirmed to be same by weighing dried slices in another experiment under same condition. The radioactivity of the tracer in each slice was measured with a liquid scintillation counter (Aloka Model, LSC-3500) for HTO and ^{36}Cl, or with an NaI scintillation counter (Aloka Model, ARC-380) for ^{134}Cs. Radioactive tracers, HTO and ^{36}Cl, were obtained from the Japan Radioisotope Association, and ^{134}Cs was prepared by neutron-irradiation of CsCl powder at the Kyoto University Research Reactor (KUR).

2.2.2. Steady-state diffusion experiment

Steady-state diffusion experiments were carried out for tracers of HTO and ^{137}Cs (total Cs concentration was 1 mM), separately, using the diffusion apparatus illustrated in Fig. 2. The bentonite sample was 20-mm diameter by 20-mm thick for HTO and 5-mm thick for ^{137}Cs, and was placed between two solution cells to allow tracer in a cell to diffuse through the bentonite sample to the other cell. The volume of solution in both cells, tracer and tracer-free, was 100 cm^3. The temperature of the apparatus was kept at 298 K during diffusion. The tracer concentrations in the cells were periodically measured by sampling 0.5 cm^3 of solutions. The tracer concentration in the tracer cell was controlled to be within ±15% of initial value at the early stage of the experiment, but less than ±10% after steady-state diffusion was established. On the other hand, there was no need to control the concentration in the tracer-free cell since it did not reach to 10% of the initial values in the tracer cell at the end of experiments. When the addi-

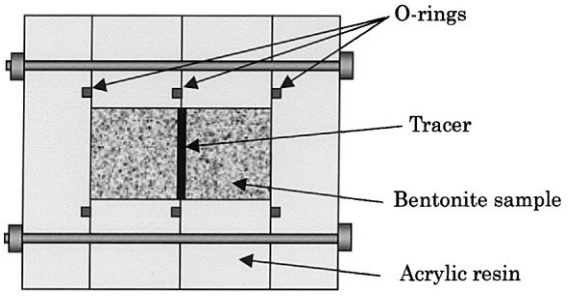

Fig. 1. Schematic outline of the non-steady state diffusion experiment.

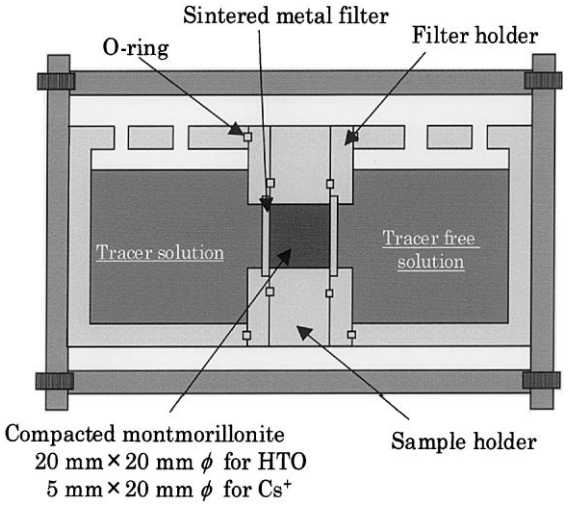

Fig. 2. Schematic outline of the steady-state diffusion experiment.

tional tracer solution was introduced into the tracer cell, same volume of distilled water was added into tracer-free cell to keep the same water levels in both cells. A Radioactive tracer, ^{137}Cs, was obtained from the Japan Radioisotope Association.

3. Results and discussion

3.1. Characteristics of bentonite

Bentonite particles consist of largely continuous stacks of montmorillonite flakes, of which unit structure is 2:1 layer of silicate with about 1 nm thickness. Exchangeable cations exist between stacking unit layers to compensate excess electrical charge on the layers. Therefore, in addition to the external surfaces, bentonite particles have the inner surfaces in interlayer where the flakes sandwich exchangeable cations.

Specific surface areas of the two different particle size samples determined by the BET and the EGME methods are listed in Table 1. The specific surface area obtained by the EGME method was more than ten times larger than that by the BET method, since the EGME method can measure the inner surface areas in addition to the external surface areas, while the BET method can measure only the external surface areas. It is remarkable that the BET method gave a higher specific surface area for the fine grained sample than for the coarse sample, whereas same values for the specific surface areas were obtained by the EGME method. It may therefore be assumed that the montmorillonite layers, which compose the bentonite particles, have substantially similar sizes in this study, even if the particle size of the samples was different.

Table 1
Specific surface areas of bentonite samples with different particle sizes determined by BET and EGME

Particle size (μm)	BET method (m^2g^{-1})	EGME method (m^2g^{-1})
75–150	45	7.0×10^2
<45	62	7.0×10^2

Fig. 3 shows the particle size distribution of the bentonite samples determined with the particle size analyzer using ethanol as dispersion medium. The particle size of the coarse grained sample mainly distributes around 150 μm, while that of the fine grained sample mainly distributes around 20 and 40 μm. The differences in particle size agree well with the SEM observations as shown in Figs. 4 and 5. Very similar particle size distributions were obtained for the samples dispersed in water with $Na_6(PO_3)_6$, as shown in Fig. 6. It can be considered that the bentonite particles kept their geometry when dispersed in ethanol, although they decomposed when dispersed in water with $Na_6(PO_3)_6$. This observation supports the above assumption that the size

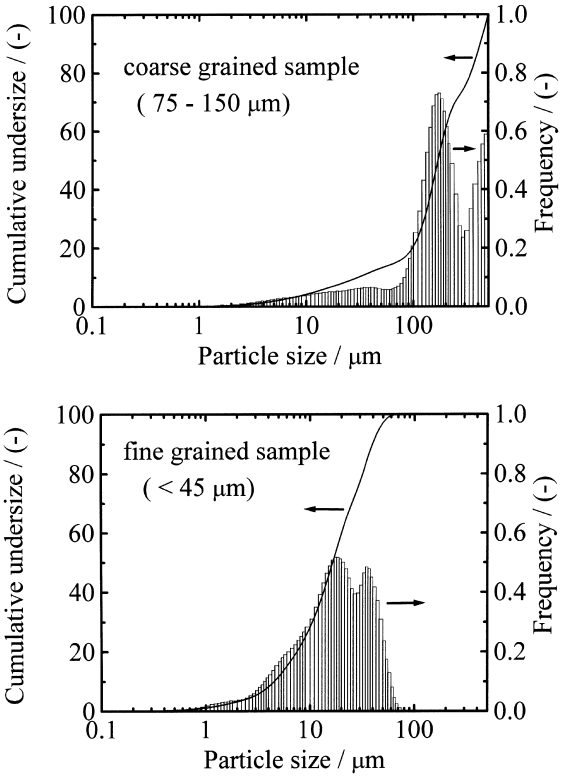

Fig. 3. Particle size distribution of bentonite samples dispersed in ethanol.

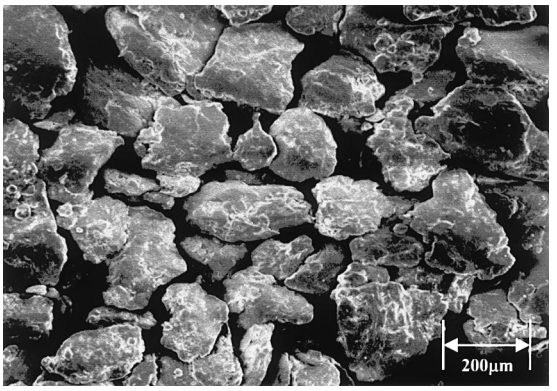

Fig. 4. SEM micrograph of coarse grained bentonite sample.

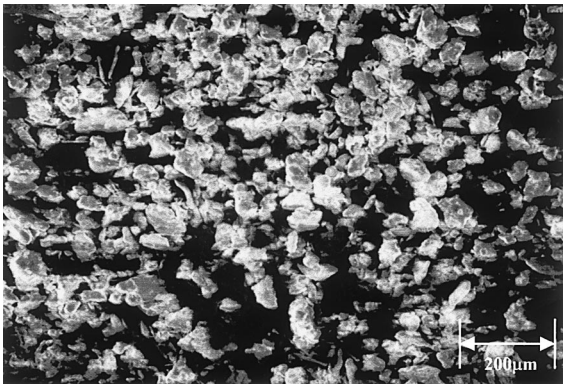

Fig. 5. SEM micrograph of fine grained bentonite sample.

of the montmorillonite layers are the same even when the particle size of the samples are different.

3.2. Diffusion coefficients

A typical concentration profile obtained in the non-steady-state diffusion experiments is shown in Fig. 7. Apparent diffusion coefficients were determined from the concentration profiles by using the following equation [21]:

$$C(x,t) = \frac{M}{2\sqrt{\pi D_a t}} \exp\left(-\frac{x^2}{4D_a t}\right), \quad (1)$$

where D_a is the apparent diffusion coefficient of the tracer in the compacted bentonite ($m^2\ s^{-1}$), C the concentration of the diffusing tracer (count m^{-3}), M the amount of the applied tracer per unit area (count m^{-2}), t the diffusion time (s), x the distance from the bentonite surface on which the tracer is spiked (m).

To establish the reproducibility of the measurements, the experiments were carried out repeatedly under the same conditions for each of the tracers, HTO, ^{36}Cl, and

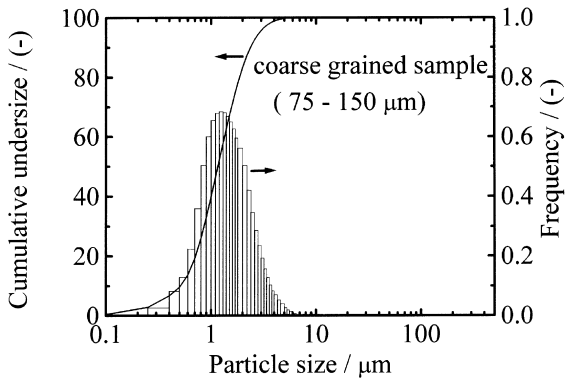

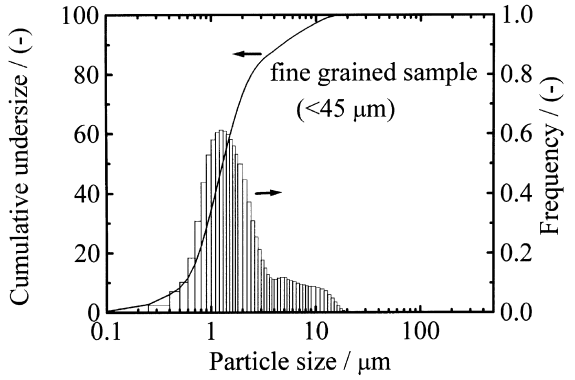

Fig. 6. Particle size distribution of bentonite samples dispersed in water with $Na_6(PO_3)_6$.

^{134}Cs. Fig. 8 shows the apparent diffusion coefficients of HTO, Cl^- ions, and Cs^+ ions determined for the two bentonite samples with different particle sizes with dry densities of 1.0 and 1.8 Mg. The average values of the apparent diffusion coefficients and the confidence intervals (calculated from n measurements for each case with the confidence limit of 95%) are all listed in Table 2. The apparent diffusion coefficients of HTO and Cl^- ions for the fine grained sample were higher than those for the coarse grained sample. According to the pore water diffusion model, the apparent diffusion coefficient can be expressed by the following equation [5]:

$$D_a = \frac{D_p \varepsilon}{\varepsilon + \rho K_d} = \frac{D_e}{\varepsilon + \rho K_d}, \quad (2)$$

where D_p is the diffusion coefficient in pore water ($m^2\ s^{-1}$), ε the porosity (–), ρ the dry density of bentonite (Mg m^{-3}), K_d the distribution coefficient (Mg m^{-3}), D_e the effective diffusion coefficient ($m^2\ s^{-1}$).

With non-sorbing nuclides such as HTO and Cl^- ions, distribution coefficients are considered negligible (K_d can be assumed to be zero), and the following equations are obtained from Eq. (2):

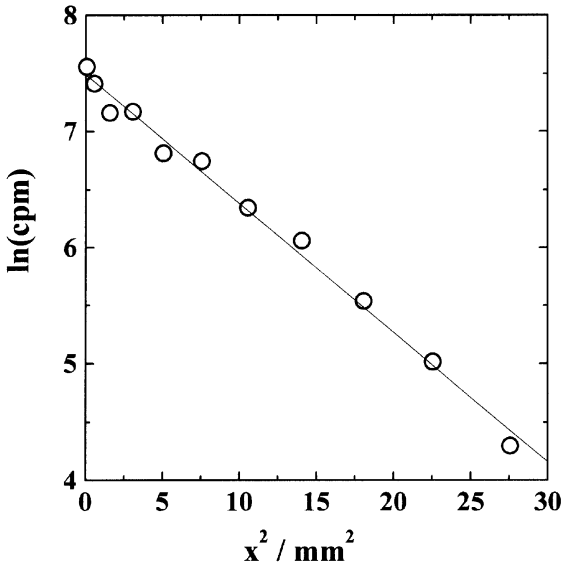

Fig. 7. Concentration profile of ^{134}Cs in compacted bentonite(coarse grained) in the non-steady diffusion experiment; dry density: 1.8 Mg m^{-3}, diffusion temperature: 298 K, diffusion duration: 477 h, apparent diffusion coefficient: 1.38×10^{-12} m^2 s^{-1}.

$$D_a = D_p = D_0 f, \tag{3}$$

$$D_e = D_p \varepsilon = D_0 f \varepsilon = \varepsilon D_a, \tag{4}$$

where D_0 is the diffusion coefficient in free water (m^2 s^{-1}), f the formation factor (−).

From Eq. (3), the formation factor for HTO and Cl^- ions can be calculated using D_0 (2.44×10^{-9} m^2 s^{-1} for HTO [22] and 2.03×10^{-9} m^2 s^{-1} for Cl^- ions [23]) and the measured D_a. Table 3 lists the formation factors obtained in this study. The smaller values of formation factor were obtained for Cl^- ions as compared to HTO at both dry densities. In conventional diffusion model, these smaller values of the formation factors for Cl^- ions are explained by effect of 'anion exclusion'; anions were repelled by electrostatic force from montmorillonite surface where negatively charged, and diffusion pathway only for anions comes to be limited [17].

The formation factors of the fine grained samples are larger than those of the coarse samples at dry densities of 1.0 and 1.8 Mg m^{-3}. After the water saturation of the sample, montmorillonite particles expand and come to contact each other, and also some particles could be dispersed in pore water as smaller particle. In this study, however, there is a particle size effect on the formation factor in the compacted bentonite even after the bentonite was saturated with water. This experimental result can mean that many particles substantially kept their original size [24], and support the pore water diffusion model.

In the steady-state diffusion experiments, the effective diffusion coefficients were determined from the time dependence of the total amount of tracer passing through the bentonite sample, using the following equation [7]:

$$C_t = \frac{ALC_0}{V}\left[\frac{D_e}{L^2}t - \frac{\alpha}{6}\right], \tag{5}$$

where C_t is the concentration of diffusing tracer in measurement tank (kg m^{-3}), C_0 the concentration of diffusing tracer in tracer tank (kg m^{-3}), V the volume of solution (m^3), L the thickness of bentonite sample (m), A the cross section of bentonite sample (m^2), α the sorption capacity factor $= \varepsilon + (1 - \varepsilon)\rho K_d$ (−).

As an example, the total amount of tracer passing through the bentonite sample is shown in Fig. 9 as a function of time. The measured effective diffusion coefficients of HTO and Cs^+ ions obtained in this study are listed in Table 4. The measured effective diffusion coefficients in the fine grained samples were slightly higher than those in the coarse grained samples for HTO. The effective diffusion coefficients of HTO were also independently calculated from the apparent diffusion coefficients of HTO using Eq. (4). The results of the calculations are also listed in Table 4. The measured and calculated values of the effective diffusion coefficients agree well at the dry density of 1.0 Mg m^{-3}, but are very different at the dry density of 1.8 Mg m^{-3}. This suggests that the pore water diffusion model is only valid for the dry density of 1.0 Mg m^{-3}. Torikai et al. [25] studied the thermodynamic properties of water in compacted bentonite, and reported that there was no free water, like pore water, at high dry densities of 1.2 Mg m^{-3} and above. It is possible that the differences in the effective diffusion coefficients at the dry density of 1.8 Mg m^{-3} can be attributed to the disappearance of the pore water, that would result in change of predominant diffusion pathway from pore water into external or internal surfaces. If this were the case, the effective diffusion coefficient, which is based on the pore water diffusion model, is not adequate for description of diffusion behavior at this dry density.

With Cs^+ ions, the particle size effect was opposite to the results with HTO and Cl^- ions; both the apparent and the effective diffusion coefficients for the fine grained sample were slightly lower than those for the coarse sample. According to the pore water diffusion model, both the apparent and the effective diffusion coefficients of Cs^+ ions are affected by changes in the formation factor by Eqs. (3) and (4). On the other hand, the radii of the chemical species of tracers could have influence on the formation factor when the tracers diffuse in a narrow tortuous path. Here we obtain almost same values of stokes radii, 120 pm, for Cs^+ ions and Cl^- ions from calculation using Stokes-Einstein equation with D_0 values of 2.11×10^{-9} and 2.03×10^{-9} m^2 s^{-1} for Cs^+ ions

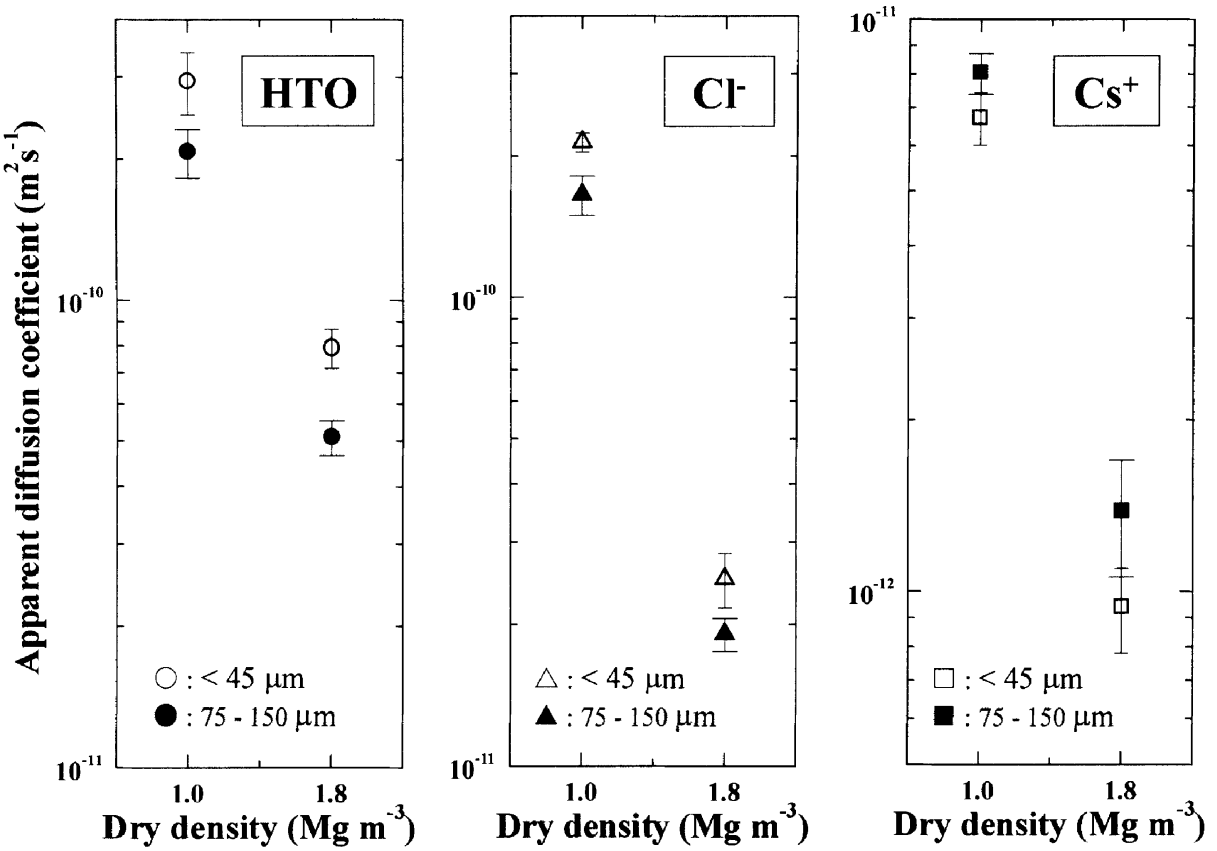

Fig. 8. Apparent diffusion coefficients of HTO, Cl^- ions, and Cs^+ ions determined for two particle sizes in bentonite samples with dry densities of 1.0 and 1.8 Mg m^{-3}.

Table 2
Average values of apparent diffusion coefficients and confidence intervals for HTO, Cl^-, and Cs^+ in compacted bentonite with different particle sizes and dry densities

Dry density (Mg m^{-3})	Particle size (μm)	Average of apparent diffusion coefficient and confidence interval		
		HTO (m^2 s^{-1})	Cl^- (m^2 s^{-1})	Cs^+ (m^2 s^{-1})
1.0	75–150	$2.07 \pm 0.25 \times 10^{-10}$ ($n=6$)	$1.65 \pm 0.16 \times 10^{-10}$ ($n=8$)	$8.04 \pm 0.67 \times 10^{-12}$ ($n=8$)
1.0	<45	$2.94 \pm 0.46 \times 10^{-10}$ ($n=6$)	$2.14 \pm 0.10 \times 10^{-10}$ ($n=9$)	$6.72 \pm 0.71 \times 10^{-12}$ ($n=12$)
1.8	75–150	$5.09 \pm 0.44 \times 10^{-11}$ ($n=6$)	$1.90 \pm 0.16 \times 10^{-11}$ ($n=8$)	$1.38 \pm 0.32 \times 10^{-12}$ ($n=7$)
1.8	<45	$7.91 \pm 0.76 \times 10^{-11}$ ($n=6$)	$2.50 \pm 0.33 \times 10^{-11}$ ($n=6$)	$9.38 \pm 1.59 \times 10^{-13}$ ($n=7$)

(n: data number).

[23] and Cl^- ions, respectively. In addition, considering the anion exclusion effect for Cl^- ions, Cl^- ions may behave as ions with largest radius among tracers used in this study. Therefore, it could be expected that the formation factor for Cs^+ ions in the fine grained sample is larger than that in the coarse sample as the case of Cl^- ions, and the diffusion coefficients increase with the formation factor when the particle size changes from coarse to fine. Contrary to this expectation, both the apparent and the effective diffusion coefficients of Cs^+ ions decreased in this study. For the apparent diffusion coefficients, the opposite particle size effect for Cs^+ ions

Table 3
The formation factors of bentonite samples calculated from the apparent diffusion coefficients of HTO and Cl^-

Dry density (Mg m^{-3})	Particle size (μm)	Porosity (–)	Formation factor (HTO) (–)	Formation factor (Cl^-) (–)
1.0	75–150	0.653	0.085	0.081
1.0	<45	0.653	0.120	0.105
1.8	75–150	0.375	0.021	0.009
1.8	<45	0.375	0.032	0.012

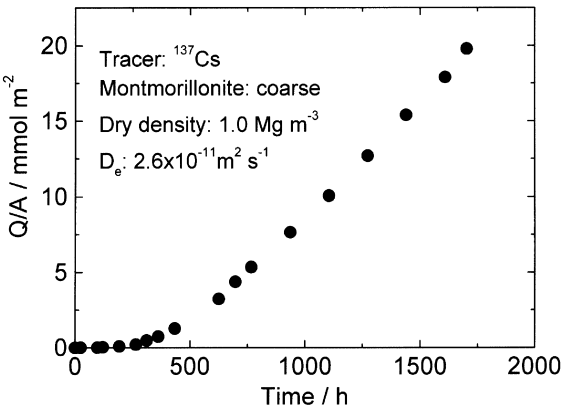

Fig. 9. Total amount of tracer passed through bentonite sample (coarse grained) as a function of time.

can be attributed to an increase in a distribution coefficient of Cs^+ ions on the bentonite, which may be caused by the increase of the BET specific surface area. However, for the effective diffusion coefficient that is independent of the distribution coefficient, there is no way to explain these findings by the pore water diffusion model.

The activation energy for diffusion is a promising parameter to clarify the diffusion process. The authors here have investigated the activation energies for the diffusion of Cs^+ [13], Sr^{2+} [14], Na^+ [15] and Cl^- [16], all as a function of the dry density. In the cases of Na^+, Sr^{2+} and Cl^-, lower activation energies than that in free water were obtained at the dry density of 1.0 Mg m^{-3}, whereas it became higher than that in free water at dry density of 1.8 Mg m^{-3}. In the case of Cs^+, although the activation energy were higher than that in free water even at the dry density of 1.0 Mg m^{-3}, it increased markedly at the dry densities of 1.4 Mg m^{-3} and above. These findings suggested the changes in the predominant diffusion process at the high dry density, and also suggested a contribution of additional diffusion processes such as diffusion on external surfaces and in interlayer. For Cs^+ ions, Berry and Bond reported an absence of surface diffusion, and suggested that the strong sorbing force of Cs^+ ions could provide strong resistance to surface diffusion [9]. It has also been reported that the diffusion coefficients of Cs^+ ions and their activation energies were remarkably affected by exchangeable cations of Ca^{2+} ions in compacted Na- and Ca-montmorillonite mixtures, and the diffusion in interlayer was considered as the most probable explanation for the findings [26].

These new concepts for the diffusion process seem to be compatible with the experimental results that were obtained in this study and cannot be explained by the pore water diffusion model; the discrepancy between the measured and the calculated effective diffusion coefficients of HTO at high dry density, and the opposite particle size effect on the formation factor of Cs^+ ions. Further investigation on this point is in progress.

4. Conclusion

The specific surface areas of bentonite samples with different particle sizes were determined by the BET and

Table 4
Effective diffusion coefficients of HTO and Cs^+ ions

Dry density (Mg m^{-3})	Particle size (μm)	Effective diffusion coefficient		
		Measured (HTO) (m^2 s^{-1})	Measured (Cs^+) (m^2 s^{-1})	Calculated from D_a (HTO) (m^2 s^{-1})
1.0	75–150	1.2×10^{-10}	2.6×10^{-11}	1.4×10^{-10}
1.0	<45	2.0×10^{-10}	1.5×10^{-11}	1.9×10^{-10}
1.8	75–150	7.3×10^{-11}	–	1.9×10^{-11}
1.8	<45	8.2×10^{-11}	–	3.0×10^{-11}

the EGME methods, and the particle size distributions of each sample were analyzed by laser diffraction/scattering particle size analysis and scanning electron microscopy. The BET method gave a higher specific surface area of the fine grained sample than of the coarse sample, while the EGME method gave similar values for both samples. The laser diffraction/scattering particle size analysis using ethanol as a dispersion medium gave different particle size distributions, but when the samples were dispersed in water with $Na_6(PO_3)_6$, the particle size distributions were similar. This indicates that the montmorillonite layers, which compose the montmorillonite particles, have the same size, even if the particle sizes of the samples are different.

The apparent and effective diffusion coefficients of HTO, Cl^- ions, and Cs^+ ions in compacted clays were determined using bentonite samples with different particle sizes and dry densities. It was found that the apparent diffusion coefficients of HTO and Cl^- for the fine grained sample were higher than for the coarse grained sample at two dry densities, 1.0 and 1.8 Mg m^{-3}, while the opposite particle size effect was observed for Cs^+ ions. These findings cannot be explained by changes in the distribution coefficients, as the effective diffusion coefficient, which is independent of the distribution factor, was also affected by the grain size of bentonite.

The new concepts for diffusion process, including the diffusion on external surfaces and interlayer, are needed for accounting the experimental results that were obtained in this study and cannot be explained by the pore water diffusion model.

Acknowledgements

A part of this work was performed in the facilities of the Central Institute of Isotope Science, Hokkaido University and the Research Reactor Institute, Kyoto University. The authors wish to thank Professor Dr H. Moriyama and Dr J. Takada, of the Research Reactor Institute, Kyoto University, and Professor Dr T. Ohnishi, of the Central Institute of Isotope Science, Hokkaido University. Financial support was provided by the Ministry of Education, Science, Sports and Culture, Japan (a Grant-in-Aid for Encouragement of Young Scientists, No.09780446), and the TEPCO Research Foundation.

References

[1] D.G. Brookins, Geochemical Aspects of Radioactive Waste Disposal, Springer, New York, 1987.
[2] Nagra, NAGRA NTB 93-22, 1994.
[3] B. Torstenfelt, SKB Tech. Rep. 86-14, Swedish Nuclear Fuel and Waste Management, 1986.
[4] I. Neretnieks, Nucl. Technol. 71 (1985) 458.
[5] H. Sato, T. Ashida, Y. Kohara, M. Yui, N. Sasaki, J. Nucl. Sci. Technol. 29 (1992) 873.
[6] H. Kim, T. Suk, S. Park, C. Lee, Waste Manage. 13 (1993) 303.
[7] A. Muurinen, P. Penttilä-Hiltunen, K. Uusheimo, Sci. Basis for Nucl. Waste Manage. XII (1989) 743.
[8] S.C.H. Cheung, M.N. Gray, ibid. XII (1989) 677.
[9] J.A. Berry, K.A. Bond, Radiochim. Acta 58&59 (1992) 329.
[10] F.M. Jahnke, C.J. Radke, US DOE Rep., LBL-20406, 1985.
[11] T.E. Eriksen, SKB Tech. Rep., Swedish Nuclear Fuel and Waste Management, 89-24, 1989.
[12] D.W. Oscarson, Clays Clay Miner. 42 (1994) 534.
[13] T. Kozaki, H. Sato, A. Fujishima, S. Sato, H. Ohashi, J. Nucl. Sci. Technol. 33 (1996) 522.
[14] T. Kozaki, H. Sato, A. Fujishima, N. Saito, S. Sato, H. Ohashi, Sci. Basis for Nucl. Waste Manage. XX (1997) 893.
[15] T. Kozaki, A. Fujishima, S. Sato, H. Ohashi, Nucl. Technol. 121 (1998) 63.
[16] T. Kozaki, N. Saito, A. Fujishima, S. Sato, H. Ohashi, J. Contaminant Hydrology 35 (1999) 67.
[17] A. Muurinen, VTT Publications 168, 1994.
[18] H. Kato, M. Muroi, N. Yamada, H. Ishida, H. Sato, Sci. Basis for Nucl. Waste Manage. XVIII (1994) 277.
[19] H. Sato, M. Yui, H. Yoshikawa, ibid. XVIII (1994) 269.
[20] I.M. Eltantawy, P.W. Arnold, J. Soil Sci. 24 (1973) 232.
[21] J. Crank, The Mathematics of Diffusion, 2nd ed., Clarendon, Oxford, 1975.
[22] J.H. Wang, C.V. Robinson, I.S. Edelman, J. Am. Chem. Soc. 75 (1953) 466.
[23] R. Parsons, Handbook of Electrochemical Constants, Butterworths, London, 1959, p. 79.
[24] R. Pusch, O. Karnland, A. Muurinen, SKB Tech. Rep. 89-34, Swedish Nuclear Fuel and Waste Management, 1989.
[25] Y. Torikai, S. Sato, H. Ohashi, Nucl. Technol. 115 (1996) 73.
[26] T. Kozaki, H. Sato, S. Sato, H. Ohashi, Proc. workshop on 'Microstructural modelling of natural and artificially prepared clay soils with special emphasis on the use of clays for waste isolation', Lund, Sweden, 12–14 Oct. 1998, p. 214.